Hydrolysis and Methanolysis of PF_4^- and Nuclear Magnetic Resonance and Vibrational Spectra of the POF_2^- and HPO_2F^- Anions†

Karl O. Christe,*[1] David A. Dixon,[2] Jeremy C. P. Sanders,[3] Gary J. Schrobilgen,*[3] and William W. Wilson[1]

Rocketdyne, A Division of Rockwell International Corporation, Canoga Park, California 91309, Department of Chemistry, McMaster University, Hamilton, Ontario L8S 4M1, Canada, and The DuPont Company, Central Research and Development, Experimental Station, Wilmington, Delaware 19880–0328

Received May 20, 1994®

The hydrolysis and methanolysis of $N(CH_3)_4PF_4$ were studied by multinuclear NMR and vibrational spectroscopy. With an equimolar amount of water in CH_3CN solution, PF_4^- forms HPO_2F^- and HPF_5^- in a 1:1 mole ratio. With an excess of water, HPO_2F^- is the sole product which was also obtained by the hydrolysis of HPF_5^-. In the presence of a large excess of F^-, the hydrolysis of PF_4^- with an equimolar amount of water produces POF_2^-. The resulting $N(CH_3)_4POF_2$ is the first known example of a stable POF_2^- salt. The geometries and vibrational spectra of POF_2^- and HPO_2F^- were calculated by *ab initio* methods, and normal coordinate analyses were carried out for POF_2^-, HPO_2F^-, and the isoelectronic SOF_2, HSO_2F, and $ClOF_2^+$ species. The F^- affinities of FPO, HPO_2, and related species and the reaction enthalpies of the hydrolysis reactions of the PF_4^- and HPF_5^- anions were also calculated by *ab initio* methods and are in accord with the experimental data. The methanolysis of PF_4^- produces $PF_2(OCH_3)$ and $PF(OCH_3)_2$ as the main products.

Introduction

$N(CH_3)_4{}^+PF_4{}^-$, the first example of a PF_4^- salt, was recently prepared and characterized in our laboratories.[4] In the course of this work, we observed that this salt undergoes very interesting hydrolysis reactions. Depending on the reaction conditions, this reaction produces either POF_2^- which previously had been observed as a free ion[5a] only at low temperature by NMR spectroscopy[5b] and in an ion cyclotron resonance spectrometer,[6] or HPO_2F^- and HPF_5^-, which had previously been characterized only incompletely.[7–15] In this paper, the hydrolysis and methanolysis reactions of PF_4^- and spectroscopic data for POF_2^- and HPO_2F^- are reported. Our results on HPF_5^- have been included in a separate paper[16] discussing mutual ligand interaction effects in monosubstituted main group hexafluorides.

Experimental Section

Apparatus and Materials. The syntheses of $N(CH_3)_4PF_4$[4] and $N(CH_3)_4HPF_5$[16] have previously been described. Volatile materials were handled in a Pyrex glass vacuum line that was equipped with Kontes glass–Teflon valves and a Heise pressure gauge. Nonvolatile materials were handled in the dry nitrogen atmosphere of a glovebox. The infrared and Raman spectrometers have previously been described.[17]

Hydrolysis of $N(CH_3)_4PF_4$. In a typical experiment, $N(CH_3)_4PF_4$ (1.104 mmol) was placed in the drybox into a baked out $^3/_4$ in. o.d. Teflon–FEP ampule that contained a Teflon-coated magnetic stirring bar and was closed by a stainless steel valve. A sample of "wet" CH_3CN was made up by the addition of a known amount of H_2O to a known amount of dry CH_3CN, and the water content of the resulting solution was verified by a Karl Fischer titration. An amount of wet CH_3CN (3.155 mL) with a total water content of 1.104 mmol was pipetted inside the drybox into the ampule containing the $N(CH_3)_4PF_4$, and the resulting mixture was stirred for 1 h at room temperature. Then, all volatile material was pumped off for 12 h at 25 °C, leaving behind 198.4 mg of a white solid that was identified by NMR and vibrational spectroscopy as an equimolar mixture of $N(CH_3)_4HPF_5$ and $N(CH_3)_4HPO_2F$ (weight calculated for 0.552 mmol of $N(CH_3)_4HPF_5$ plus 0.552 mmol of $N(CH_3)_4HPO_2F$ = 197.8 mg).

Preparation of $N(CH_3)_4HPO_2F$. When the hydrolysis reaction of $N(CH_3)_4PF_4$ was repeated with a 5-fold excess of

† Dedicated to Prof. Reinhard Schmutzler on the occasion of his 60th birthday.

® Abstract published in *Advance ACS Abstracts,* September 15, 1994.

(1) Rockwell International.
(2) DuPont, contribution no. 6869.
(3) McMaster University.
(4) Christe, K. O.; Dixon, D. A.; Mercier, H. P. A.; Sanders, J. C. P.; Schrobilgen, G. J.; Wilson, W. W. *J. Am. Chem. Soc.* **1994**, *116*, 2850.
(5) (a) Although the free POF_2^- anion was unknown, the existence of the $P(O)F_2$ ligand in transition metal complexes had been well-known from the publications of R. Schmutzler and co-workers (Grosse, J.; Schmutzler, R. *Z. Naturforsch.* **1973**, *28b*, 515; *J. Chem. Soc. Dalton Trans.*, **1976**, 405 and 412; *Acta Crystallogr.* **1974**, *B30*, 1623. Neumann, S.; Schomburg, D.; Schmutzler, R. *J. Chem. Soc., Chem. Commun.* **1979**, 848. Hietkamp, S.; Schmutzler, R. *Z. Naturforsch.* **1980**, *35b*, 548. Krüger, W.; Sell, M.; Schmutzler, R. *Z. Naturforsch.* **1983**, *38b*, 1074. Plinta, H. J.; Gereke, R.; Fischer, A.; Jones, P.G.; Schmutzler, R. *Z. Naturforsch.* **1993**, *48b*, 737). (b) Ebsworth, E. A. V.; Page, P. G.; Rankin, W. H. *J. Chem. Soc., Dalton Trans.* **1984**, 2569.
(6) Larson, J. W.; McMahon, T. B. *Inorg. Chem.* **1987**, *26*, 4018; *J. Am. Chem. Soc.* **1983**, *105*, 2944.
(7) Schülke, U.; Kayser, R. *Z. Anorg. Allg. Chem.* **1991**, *600*, 221.
(8) Blaser, B.; Worms, K. H. *Z. Anorg. Allg. Chem.* **1968**, *360*, 117.
(9) Falius, H. *Angew. Chem., Int. Ed. Engl.* **1970**, *9*, 733. Ahrens, H.; Falius, H. *Chem. Ber.* **1972**, *105*, 3317.
(10) Nixon, J. F.; Swain, J. R. *Inorg. Nucl. Chem. Lett.*, **1969**, *5*, 295.
(11) Nixon, J. F.; Swain, J. R. *J. Chem. Soc. A* **1970**, 2075.
(12) McFarlane, W.; Nixon, J. F.; Swain, J. R. *Mol. Phys.* **1970**, *19*, 141.
(13) Cowley, A. H.; Wisian, P. J.; Sanchez, M. *Inorg. Chem.* **1977**, *16*, 1451.
(14) Minkwitz, R.; Liedtke, A. *Z. Naturforsch. B* **1989**, *44B*, 679.
(15) Lindemann, D.; Riesel, L. *Z. Anorg. Allg. Chem.* **1992**, *615*, 66. Riesel L.; Kant, M. *Z. Chem.* **1984**, *24*, 382.
(16) Christe, K. O.; Dixon, D. A.; Wilson, W. W. *J. Am. Chem. Soc.* In press.
(17) Christe, K. O.; Curtis, E. C.; Dixon, D. A.; Mercier, H. P.; Sanders, J. C. P.; Seppelt, K.; Schrobilgen, G. J.; Wilson, W. W. *J. Am. Chem. Soc.* **1991**, *113*, 3351.

0020-1669/94/1333-4911$04.50/0

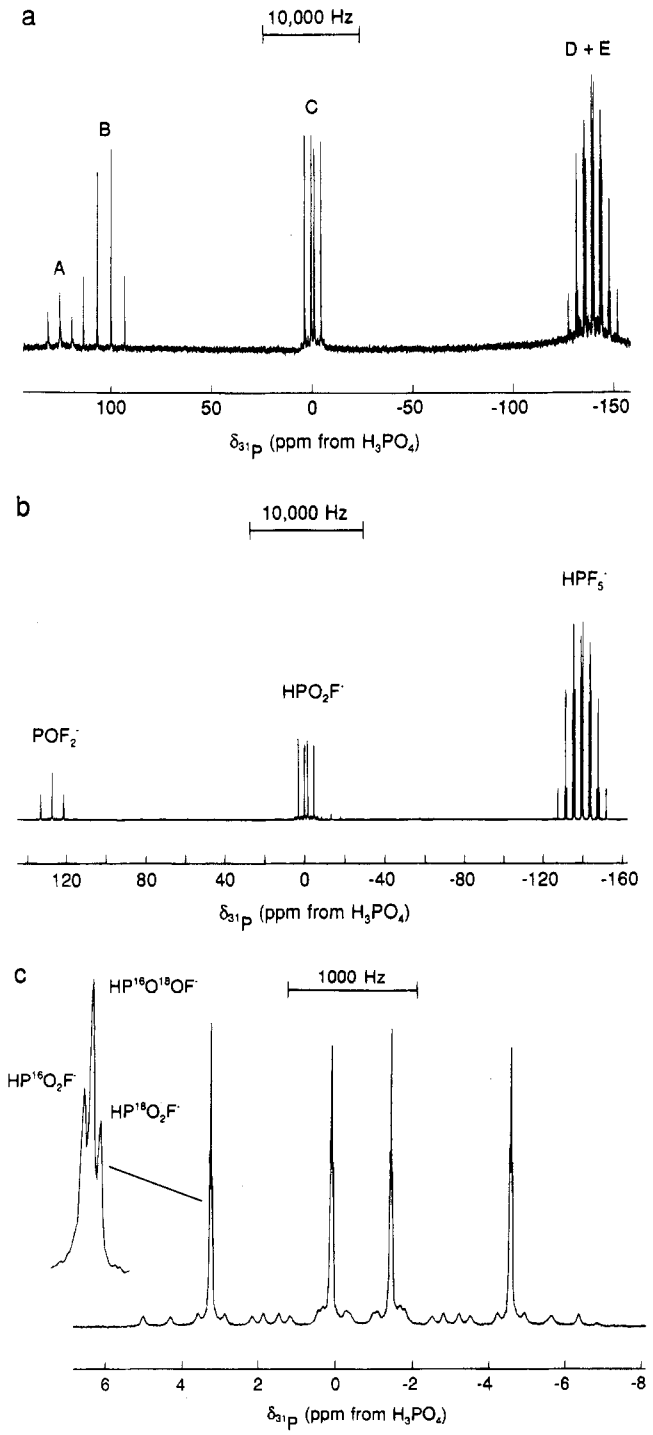

Figure 1. ^{31}P NMR spectrum (202.459 MHz) of a sample containing equimolar quantities of $N(CH_3)_4PF_4$ and H_2O (oxygen isotopic composition: ^{16}O,35.4%; ^{17}O, 21.9%; ^{18}O, 42.7%) in CH_3CN. (a) At −45 °C, (A) POF_2^-; (B) PF_3; (C) HPO_2F^-; (D) HPF_5^-; (E) $[HPF_4(OH)]^-$? (b) same region at 30 °C; (c) at 30 °C, expansion of HPO_2F^- multiplet revealing $^{16,18}O$ isotope shifts arising from the $HP^{16}O_2F^-$, $HP^{16}O^{18}OF^-$, and $HP^{18}O_2F^-$ isotopomers. The equal-intensity sextet satellites at the bases of the four main components of the multiplet arise from coupling to ^{17}O in the $HP^{16}O^{17}OF^-$ and $HP^{17}O^{18}OF^-$ isotopomers.

H_2O and a reaction time of 5 days, followed by removal of all volatile material in a dynamic vacuum at 85 °C for 2 days, the sole product was $N(CH_3)_4HPO_2F$.

Hydrolysis of $N(CH_3)_4HPF_5$. A hydrolysis reaction of $N(CH_3)_4HPF_5$ with 2 mol of H_2O was carried out at room temperature, as described above for $N(CH_3)_4PF_4$. After agitation for 16 h, the originally present white solid had completely dissolved. Removal of all volatile material at 60 °C for 15 h in a dynamic vacuum resulted in a white product consisting of $N(CH_3)_4HPO_2F$ and some unreacted $N(CH_3)_4HPF_5$.

Hydrolysis of $N(CH_3)_4PF_4$ in the Presence of $N(CH_3)_4F$. A 3/4 in. o.d. Teflon−FEP ampule that was closed by a stainless steel valve was loaded in the drybox with $N(CH_3)_4F$ (16.31 mmol). Wet CH_3CN (12.5 g), containing 4.05 mmol of H_2O, was added to the ampule, and PF_3 (4.05 mmol) was added at −196 °C on the vacuum line. The mixture was warmed to −30 °C for 1 h with agitation, and a voluminous white precipitate formed. After warming for 1 h to room temperature, all material volatile at room temperature was pumped off for 8 h, leaving behind a white solid residue (1949.4 mg, weight calculated for 4.05 mmol of $N(CH_3)_4POF_2$ + 8.10 mmol of $N(CH_3)_4HF_2$ + 4.6 mmol of $N(CH_3)_4F$ = 1946.0 mg) which, based on its infrared spectrum, was a mixture of $N(CH_3)_4POF_2$, $N(CH_3)_4HF_2$, and $N(CH_3)_4F$.

Nuclear Magnetic Resonance Measurements. Samples for ^{31}P and ^{19}F NMR spectroscopy were prepared in 9 mm and 5 mm o.d. Teflon−FEP NMR tubes, respectively, and recorded as previously described[4] on a Bruker AM-500 spectrometer. The spectra were referenced to neat external samples of $CFCl_3$ (^{19}F), 85% H_3PO_4 (^{31}P) and H_2O (^{17}O) at ambient temperature. The chemical shift convention used is that a positive sign signifies a chemical shift to high frequency of the reference compound.

(a) Reaction of $N(CH_3)_4PF_4$ with H_2O in CH_3CN. Typically, $^{17,18}O$-enriched H_2O (8.66 μL, 0.454 mmol) was injected into a 9 mm FEP tube from a microsyringe in a nitrogen-filled glovebag. The tube was closed with a Kel-F valve and attached to a glass vacuum line. Anhydrous CH_3CN (1.8 mL) was distilled *in vacuo* into the tube at-196 °C. The tube was pressurized with dry N_2 at −78 °C, allowed to warm to room temperature, and mixed well. The tube was taken into the drybox and cooled to −196 °C in a cold well. The $N(CH_3)_4PF_4$ (0.0822 g, *ca.* 0.45 mmol), containing 10−15% $N(CH_3)_4POF_2$ and $N(CH_3)_4HPF_5$ as impurities, was added on top of the frozen $^{17,18}O$-enriched H_2O/CH_3CN mixture contained in the FEP tube. The sample tube was kept at −196 °C while removing it from the drybox, heat sealing it under a dynamic vacuum, and storing it until the NMR spectra could be obtained.

(b) Reaction of $N(CH_3)_4PF_4$ with H_2O in the Presence of $N(CH_3)_4F$ in CH_3CN. These samples were prepared in a similar way to (a) using the following typical quantities: $^{17,18}O$-enriched H_2O (8.5 μL, 0.45 mmol); $N(CH_3)_4PF_4$ (containing 10−15% $N(CH_3)_4POF_2$ and $N(CH_3)_4HPF_5$ as impurities, 0.080 81 g, *ca.* 0.46 mmol); $N(CH_3)_4F$ (0.109 23 g, 1.1727 mmol). The $N(CH_3)_4F$ was added with the $N(CH_3)_4PF_4$ on top of the frozen $^{17,18}O$-enriched H_2O/CH_3CN mixture. The sample tube was kept at −196 °C until the NMR spectra could be obtained.

The ^{19}F NMR samples were prepared in an analogous fashion to the ^{31}P samples by using 4 mm o.d. FEP NMR tubes and the following typical quantities: (a) $N(CH_3)_4PF_4$ (0.0100 g, 0.0552 mmol); $^{17,18}O$-enriched H_2O (1.1 μL, 0.055 mmol) and CH_3CN (0.25 mL); (b) $N(CH_3)_4PF_4$ (0.0096 g, 0.053 mmol); $N(CH_3)_4F$ (0.0194 g, 0.208 mmol); $^{17,18}O$-enriched H_2O (1.1 μL, 0.055 mmol); CH_3CN (0.25 mL). Samples were not warmed above −78 °C until just prior to recording the spectra.

The sealed FEP sample tubes were inserted into 10 mm or 5 mm thin-walled precision NMR tubes (Wilmad) before being placed in the probe.

Computational Methods. The electronic structure calculations were done at three different levels on a Cray YMP computer. The local density functional calculations were done

Table 1. NMR Parameters for the HPF_5^-, HPO_2F^-, and POF_2^- Anions Produced in the Hydrolysis of $N(CH_3)_4PF_4$

anion	temp, °C	$\delta(^{31}P)$, ppm	$\delta(^{19}F)$, ppm	$\delta(^{17}O)$, ppm	$^1J(^{31}P-^{19}F)$, Hz	$^1J(^{31}P-^{17}O)$, Hz	$^1J(^{31}P-^1H)$, Hz	$^2J(^1H-^{19}F)$, Hz
HPF_5^- [a]	30	−140.2	−66.6 (F_a)		731 (F_a)		939	
			−55.8 (F_e)		817 (F_e)			127 (F_e)
HPO_2F^-	30[b]	−0.7	−53.6	131.8[c]	947	145	636	127
	−36[b]			117		131		
	−45[b]	−0.5			967		684	
	30[d]			136.4		148		
POF_2^-	30[b]	127.2	−7.5	191.4	1200	187		
	30[d]	129.1		211.9	1183	189		
	−45[d]	129.4		211.8	1184			

[a] F_a and F_e refer to the axial and equatorial fluorine ligand environments, respectively; $^2J(F_a-F_e) = 42$ Hz. The NMR parameters of HPF_5^- exhibited only a very small temperature and F^- ion dependence between 30 °C and −45 °C. [b] No $N(CH_3)_4F$ added. [c] $^2J(^{17}O-^{19}F) \approx {}^2J(^{17}O-^1H) \approx 11.8$ Hz. [d] Recorded in the presence of a 2.6 molar excess of $N(CH_3)_4F$.

with the program DMol as previously described[18] with a polarized double numerical basis set (LDFT/DNP). Gradient corrected or nonlocal density functional calculations were done with the program DGauss[19] which employs Gaussian basis sets. The basis sets for the atoms are triple ζ in the valence space augmented with a set of polarization functions (TZVP).[20] These calculations were done at the self-consistent gradient-corrected (nonlocal) level (NLDFT) with the nonlocal exchange potential of Becke[21] together with the nonlocal correlation functional of Perdew[22] (BP). The *ab initio* molecular orbital (MO) theory calculations were done at the Hartree−Fock level with the program GRADSCF[23] with a polarized double ζ basis set augmented by polarization and diffuse (p on heavy atoms and s on H(ζ(s) = 0.041)) functions.[24] Geometries at all levels were optimized by using analytical gradients.[19,25] The second derivatives for the DFT calculations were calculated by numerical differentiation of the analytic first derivatives. A two-point method with a finite difference of 0.01 au was used. Analytical second derivatives were used for the MO calculations.[25]

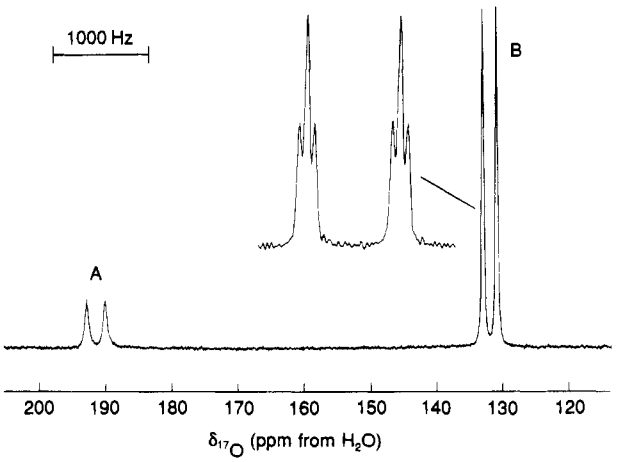

Figure 2. ^{17}O NMR spectrum (67.801 MHz) of the same sample as in Figure 1 at 30 °C. (A) POF_2^-; (B) HPO_2F^-. Insert shows a resolution-enhanced expansion of the HPO_2F^- multiplet and displays the fine structure arising from the $^2J(^{17}O-^1H)$ and $^2J(^{17}O-^{19}F)$ couplings which have similar magnitudes (≈12 Hz).

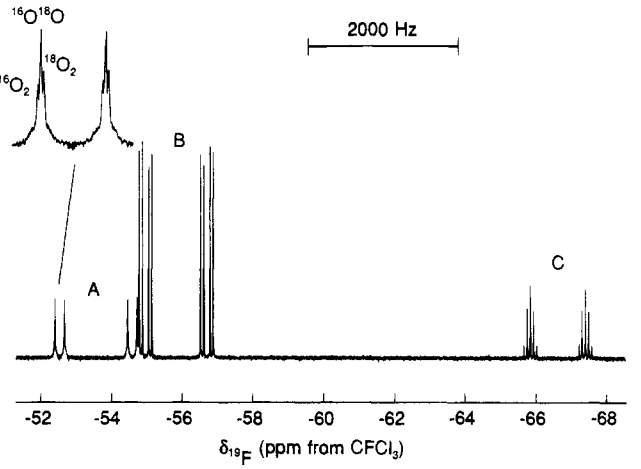

Figure 3. ^{19}F NMR spectrum (470.599 MHz) of the same sample as in Figure 1 at 30 °C. (A) HPO_2F^-; (B) F_{eq} HPF_5^-; (C) F_{ax} HPF_5^-. Expansion displays two-bond $^{16,18}O$ isotope shifts arising from the $HP^{16}O_2F^-$, $HP^{16}O^{18}OF^-$, and $HP^{18}O_2F^-$ isotopomers.

Results and Discussion

The hydrolysis of PF_4^- in CH_3CN solution was studied by multinuclear NMR and vibrational spectroscopy. As shown in the following paragraphs, the nature of the formed products strongly depends on the stoichiometry of the reagents and the reaction conditions.

Hydrolysis of PF_4^- with Equimolar Amounts of Water. The hydrolysis of PF_4^- with an equimolar amount of water in CH_3CN solution at ambient temperature proceeds rapidly and almost quantitatively according to eq 1

(18) (a) Christe, K. O.; Wilson, R. D.; Wilson, W. W.; Bau, R.; Sukumar, S.; Dixon, D.A. *J. Am. Chem. Soc.* **1991**, *113*, 3795. (b) Dixon, D. A.; Andzelm. J.; Fitzgerald, G.; Wimmer, E.; Jasien, P. In *Density Functional Methods in Chemistry*; Labanowski, J., Andzelm, J., Eds.; Springer Verlag: New York, 1991; p 33. (c) Dixon, D. A.; Christe, K. O. *J. Phys. Chem.* **1992**, *96*, 1018. (d) Delley, B. *J. Chem. Phys.* **1990**, *92*, 508. DMol is available commercially from BIOSYM Technologies, San Diego, CA. A FINE grid was used.

(19) (a) Andzelm, J.; Wimmer, E.; Salahub, D. R. In *The Challenge of d and f Electrons: Theory and Computation*; Salahub, D. R., Zerner, M. C., Eds.; ACS Symposium Series No. 394; American Chemical Society: Washington, D. C.. 1989; p 228. (b) Andzelm, J. In *Density Functional Methods in Chemistry*; Labanowski, J., Andzelm, J., Eds.; Springer Verlag: New York, 1991; p 101. (c) Andzelm, J. W.; Wimmer, E. *J. Chem. Phys.* **1992**, *96*, 1280. DGauss is a local density functional program available via the Cray Unichem Project.

(20) Godbout, N.; Salahub, D. R.; Andzelm, J.; Wimmer, E. *Can. J. Chem.* **1992**, *70*, 560.

(21) (a) Becke, A. D. *Phys. Rev. A* **1988**, *38*, 3098. (b) Becke, A. D. In *The Challenge of d and f Electrons: Theory and Computation*; Salahub, D. R., Zerner, M. C., Eds.; ACS Symposium Series No. 394; American Chemical Society: Washington, D. C., 1989, p 166. (c) Becke, A. D. *Int. J. Quantum Chem. Quantum. Chem. Symp.* **1989**, *23*, 599.

(22) Perdew, J. P. *Phys. Rev. B* **1986**, *33*, 8822.

(23) (a) GRADSCF is an *ab initio* program system designed and written by A. Komornicki at Polyatomics Research. (b) Komornicki, A.; Ishida, K.; Morokuma, K.; Ditchfield, R.; Conrad, M. *Chem. Phys. Lett.* **1977**, *45*, 595. (c) McIver, J. W., Jr.; Komornicki, A. *Chem. Phys. Lett.* **1971**, *10*, 202. (d) Pulay, P. In *Applications of Electronic Structure Theory*; Schaefer, H. F., III, Ed.; Plenum Press: New York, 1977; p 153. (e) King, H. F.; Komornicki, A. *J. Chem. Phys.* **1986**, *84*, 5465. (f) King, H. F.; Komornicki, A. In *Geometrical Derivatives of Energy Surfaces and Molecular Properties*; Jorgenson, P., Simons, J., Eds.; NATO ASI Series C. Vol. 166; D. Reidel: Dordrecht, 1986; p 207.

(24) (a) Dunning, T. H., Jr.; Hay, P. J. In *Methods of Electronic Structure Theory*, Schaefer, H. F., III, Ed.; Plenum Press: New York, 1977; Chapter 1 for F, H and O basis sets and for diffuse functions. (b) McLean, A. D.; Chandler, G. S. *J. Chem. Phys.* **1980**, *72*, 5639 for P, S, and Cl basis sets.

(25) See refs 23b−f.

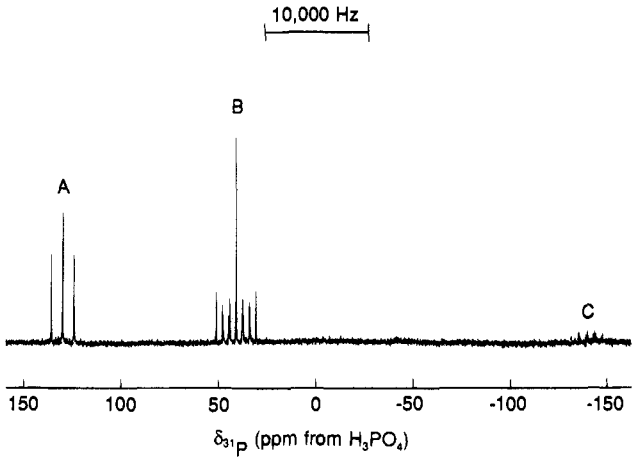

Figure 4. ^{31}P NMR spectrum (202.459 MHz) of a sample containing equimolar quantities of $N(CH_3)_4PF_4$ and H_2O (oxygen isotopic composition: ^{16}O, 35.4%; ^{17}O, 21.9%; ^{18}O, 42.7%) and a 2.6 molar excess of $N(CH_3)_4F$ in CH_3CN at −45 °C. (A) POF_2^-; (B) PF_4^-; (C) HPF_5^-.

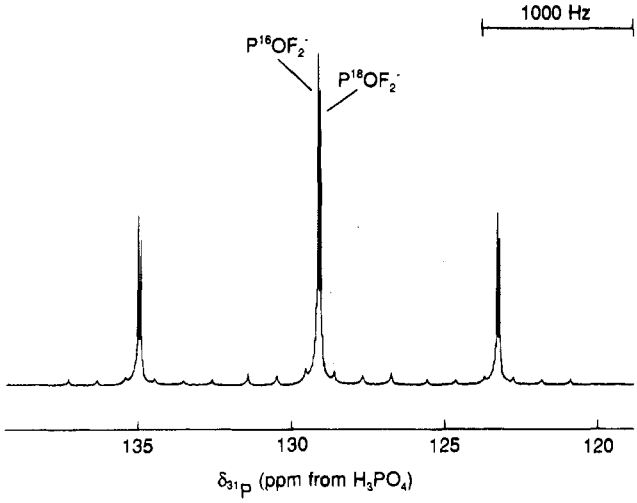

Figure 5. ^{31}P NMR spectrum (202.459 MHz) of the same sample as in Figure 4 at 30 °C. Expansion of POF_2^- multiplet revealing $^{16,18}O$ isotope shifts arising from the $P^{16}OF_2^-$ and $P^{18}OF_2^-$ isotopomers. The equal-intensity sextet satellites at the bases of the three main components of the multiplet arise from coupling to ^{17}O in the $P^{17}OF_2^-$.

$$2PF_4^- + 2H_2O \xrightarrow[20\ °C]{CH_3CN} HPO_2F^- + HPF_5^- + 2HF \quad (1)$$

This result was confirmed by multinuclear NMR spectroscopy.

The ^{31}P NMR spectrum of a sample containing equimolar quantities of $N(CH_3)_4PF_4$ and H_2O (oxygen isotopic composition: ^{16}O, 35.4%; ^{17}O, 21.9%; ^{18}O, 42.7%) in CH_3CN at −45 °C is shown in Figure 1a and reveals five resonances. Three of these resonances, A, C, and D, are assigned to the POF_2^-,[5] HPO_2F^-,[7-9] and HPF_5^-,[10-15] anions, respectively, and their NMR data are collected in Table 1. The weak quartet at high frequency, B, is assigned to PF_3 [δ = 103.5 ppm; $^1J(^{31}P-^{19}F)$ = 1401 Hz] by comparison with the literature data.[26] A very weak multiplet, E, was also observed overlapping with the HPF_5^- resonance. Since the resonance occurs in the hexacoordinate P(V) region of the spectrum, it is tentatively assigned to the $[HPF_4(OH)]^-$ anion which is a proposed intermediate in the hydrolysis reaction (see below). Although the HPO_2F^- and

(26) Gutowsky, H. S.; McCall, D. W.; Slichter, C. P. *J. Chem. Phys.* **1953**, *21*, 279. Gutowsky, H. S.; McCall, D. W.; Slichter, C. P. *J. Chem. Phys.* **1954**, *22*, 162. Martin, D. R.; Pizolato, P. J. *J. Am. Chem. Soc.* **1950**, *72*, 4584.

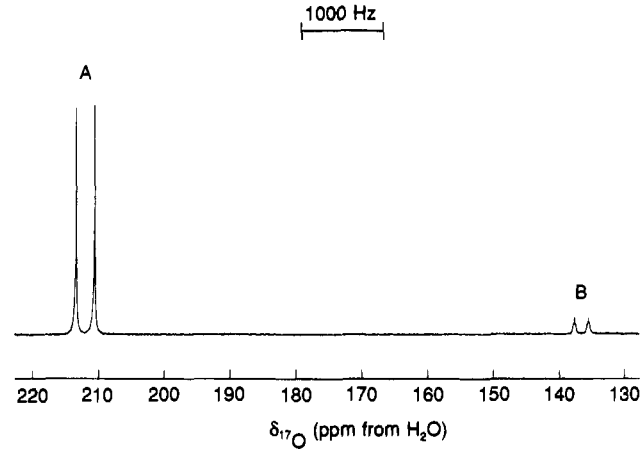

Figure 6. ^{17}O NMR spectrum (67.801 MHz) of the same sample as in Figure 4 at 30 °C: (A) POF_2^-; (B) HPO_2F^-.

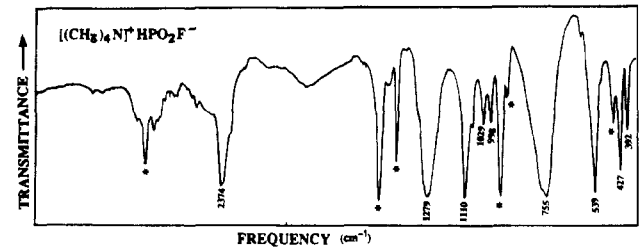

Figure 7. Infrared spectrum of solid $N(CH_3)_4HPO_2F$ recorded as an AgBr disk at room temperature. The bands marked by an asterisk are due to $N(CH_3)_4^+$, and their assignments have previously been discussed in ref 17.

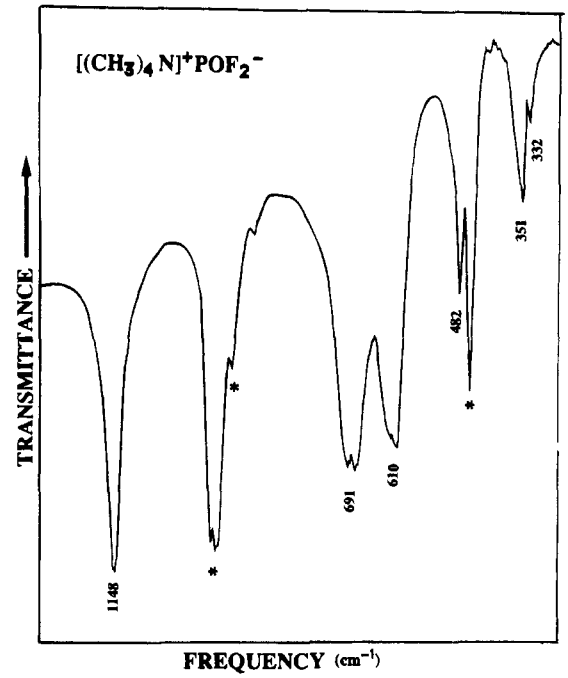

Figure 8. Infrared spectrum of solid $N(CH_3)_4POF_2$ recorded as an AgBr disk at room temperature. The bands marked by an asterisk are due to $N(CH_3)_4^+$.

POF_2^- anions had been reported previously,[7-15] prior to the present study these anions had not been fully characterized in solution by multi-NMR spectroscopy. The formation of $^{17,18}O$-enriched HPO_2F^- and POF_2^- in our studies has allowed unequivocal identification of these two anions by the observation of the ^{17}O NMR spectra as well as the $^{16,18}O$-induced secondary isotopic shifts in the ^{31}P NMR spectra (see below). The small amount of POF_2^- observed in the spectrum was

Table 2. Calculated Geometries of HPO_2F^- and HSO_2F

	HPO_2F^-			HSO_2F		
	LDFT	NLDFT/TZVP	HF/DZP+	LDFT	NLDFT/TZVP	HF/DZP+
r_{XO}, Å	1.506	1.514	1.474	1.444	1.456	1.407
r_{XF}, Å	1.661	1.679	1.609	1.612	1.643	1.549
r_{XH}, Å	1.437	1.444	1.401	1.371	1.379	1.326
∠OXO or FXF, deg	125.6	125.2	123.9	125.2	124.5	123.4
∠OXH, deg	106.8	106.7	107.1	107.1	107.0	107.7
∠OXH, deg	109.2	109.5	109.5	109.2	109.8	109.9
∠FXH, deg	94.5	94.9	96.0	94.6	94.4	95.8

Table 3. Calculated and Experimental Geometries for the Isoelectronic Series POF_2^-, SOF_2, and $ClOF_2^+$

	POF_2^-			SOF_2				$ClOF_2^+$		
	LDFT	NLDFT/TZVP	HF/DZP+	LDFT	NLDFT/TZVP	HF/DZP+	exp[a]	LDFT	NLDFT/TZVP	HF/DZP+
r_{XO}, Å	1.522	1.522	1.481	1.456	1.457	1.409	1.413	1.431	1.440	1.374
r_{XF}, Å	1.717	1.733	1.653	1.647	1.657	1.570	1.585	1.625	1.652	1.535
∠FXF, deg	90.8	91.2	91.4	92.7	92.9	92.5	92.83	94.9	95.6	93.4
∠OXF, deg	105.3	105.6	105.0	106.8	107.0	106.4	106.82	109.6	109.2	108.8

[a] Data from ref 31.

Table 4. Vibrational Frequencies of HPO_2F^- and HSO_2F

assignment in point group C_s	approximate mode description	HPO_2F^- obsd,[a] cm^{-1} (int)		HPO_2F^- calcd (IR int)			HSO_2F calcd (IR int)[f]		
		IR	RA	LDFT[b]	NLDFT/TZVP[d]	HF/DZP+[e]	LDFT	NLDFT/TZVP	HF/DZP+
A′ ν_1	νXH	2374 s	2370(2.4)	2352	2376(248)	2321(312)	2634	2615(24)	2646(19)
ν_2	ν sym XO_2	1110 s	1110(10)	1114	1128(147)	1098(236)	1220	1220(113)	1213(193)
ν_3	δ sciss HXF	998 w	1000 (0.3)	1006	1013(23)	1076(50)	1095	1074(2.2)	1125(5.9)
ν_4	νXF	755 vs	754[c]	728	710(213)	732(269)	803	753(206)	833(262)
ν_5	δ rock XO_2	539 ms	540(1)	550	533(59)	540(119)	603	565(54)	591(102)
ν_6	δ sciss XO_2	427 m	427(0+)	425	419(14)	421(33)	466	449(10)	466(32)
A″ ν_7	ν asym XO_2	1279 vs	1281 (0.5)	1342	1341(358)	1280(544)	1485	1466(260)	1428(425)
ν_8	δ wag XH	1029 w	1029(0.5)	1023	1049(20)	1061(45)	1121	1126(2.0)	1159(8.4)
ν_9	δ wag XF	392 mw		384	392(7.4)	384(14)	417	412(13)	464(23)

[a] Frequencies are for the solid $N(CH_3)_4^+$ salt from this study. The following infrared bands have previously been reported in ref 9. $Li(HPO_2F)$: 2462 vs, 1247 vs, 1137 vs, 1053 s, 1010 vs, 857 vs, 565 s, 479 s, 372 s. $Li(DPO_2F)$: 1747 s, 1241 vs, 1140 vs, 855 vs, 776 s, 742 s, 560 s, 478 s, 381 s. [b] Empirical scaling factors used to maximize the fit between observed and calculated frequencies: stretching modes, 1.039; deformation modes, 1.121. [c] Coincides with intense $\nu_3(A_1)$ band of $N(CH_3)_4^+$. [d] Empirical scaling factors of 1.0699 and 1.0890 were used for the stretching and deformation modes, respectively. [e] An empirical scaling factor of 0.9133 was used. [f] The same scaling factors were used as for HPO_2F^-.

present as an impurity in the $N(CH_3)_4PF_4$ starting material used to prepare the NMR sample and was not generated by the hydrolysis as shown by the ^{17}O NMR spectrum at −36 °C. This spectrum displayed only a broad doublet ($\Delta\nu_{1/2}$ = 76 Hz) due to HPO_2F^- and no resonance ascribable to POF_2^-.

When the ^{31}P NMR spectrum was recorded at 30 °C, the hydrolysis had gone to completion and all the PF_3 had disappeared (Figure 1b). The ^{31}P, ^{19}F, and ^{17}O NMR data for the observed species are also given in Table 1. The resonance due to POF_2^- had become somewhat more intense and now displayed ^{17}O satellites, thereby indicating a small amount of side reaction in which POF_2^- was produced. Each component of the doublet of doublets (resonance C and Figure 1c) arising from HPO_2F^- was now resolved into three lines which correspond to the $^{16,18}O$-induced secondary isotopic shifts for the three isotopomers $HP^{16}O_2F^-$, $HP^{16}O^{18}OF^-$, and $HP^{18}O_2F^-$. The isotopic shift $^1\Delta^{31}P(^{18,16}O)$ was measured as −0.0358 ± 0.0008 ppm. The observation of these three isotopomers proves that the anion has two oxygen atoms bonded to phosphorus. In addition, each component displayed well resolved, equal-intensity sextet satellites resulting from coupling of ^{31}P to ^{17}O (I = 5/2). The ^{17}O satellites are well-resolved at 30 °C owing to the slower rate of quadrupolar relaxation of the ^{17}O nucleus at higher temperatures. The spectrum also reveals that the weak multiplet, E, which was partially obscured by the intense HPF_5^- multiplet at −36 °C has disappeared on warming, thereby indicating that it might have arisen from the proposed $[HPF_4(OH)]^-$ intermediate (see below). The ^{17}O NMR spectrum (Figure 2) of the same sample at 30 °C shows two resonances: an intense doublet, B, assigned to HPO_2F^- and a weaker doublet, A, assigned to POF_2^-. Each component of the doublet resonance of HPO_2F^- is further split into an overlapping doublet of doublets (Figure 2) by the two-bond couplings to ^1H and ^{19}F [$^2J(^{17}O-^1H) \approx 12$ Hz; $^2J(^{17}O-^{19}F) \approx 12$ Hz].

The ^{19}F NMR spectrum at 30 °C of a sample containing equimolar quantities of $N(CH_3)_4PF_4$ and $^{17,18}O$-enriched H_2O in CH_3CN (Figure 3) reveals a doublet of doublets, A, arising from HPO_2F^-, as well as the resonances B and C attributable to the axial and equatorial fluorine ligand environments, respectively, of HPF_5^-. Under high resolution, each component of the HPO_2F^- resonance is found to comprise three lines corresponding to the three isotopomers $HP^{16}O_2F^-$, $HP^{16}O^{18}OF^-$, and $HP^{18}O_2F^-$. The two-bond isotopic shift, $^2\Delta^{19}F(^{18,16}O)$, was measured as −0.0125 ± 0.0004 ppm and, to the best of our knowledge, is the first experimentally determined $^2\Delta^{19}F(^{18,16}O)$ value. In addition, a broad unresolved hump is visible at the base of each component of the HPO_2F^- multiplet which results from the two-bond coupling of ^{19}F to ^{17}O in the $HP^{16}O^{17}OF^-$ and $HP^{18}O^{17}OF^-$ isotopomers. Attempts to observe the ^{19}F resonance of the intermediate species $HPF_4(OH)^-$ were unsuccessful owing to the difficulty in mixing the reagents and moderating the vigor of the hydrolysis reaction at −45 °C in a 4 mm FEP NMR tube.

Hydrolysis of PF_4^- with an Excess of Water. If a large excess of water is used in the hydrolysis of PF_4^- in CH_3CN solution, the originally formed HPF_5^- also undergoes slow

Table 5. Vibrational Spectra of Isoelectronic POF_2^-, SOF_2, and $ClOF_2^+$

assignment in point group C_s	approximate mode description	POF_2^-					SOF_2					$ClOF_2^+$				
		obsd[a]		calcd			obsd[c]		calcd (IR int)			obsd[j]		calcd		
		IR	RA	LDFT[b]	NLDFT/TZVP[c]	HF/DZP+[d]	IR	RA	LDFT[f]	NLDFT/TZVP[g]	HF/DZP+[h]	IR	RA	LDFT[k]	NLDFT/TZVP[l]	HF/DZP+[m]
A′ ν_1	νXO	1148 vs	1146	1158	1235(184)	1165(317)	1340.8 s 1330.9 s	1339.3 vs 1329.9 vs	1333	1388(147)	1309(263)	1331 ms	1333(2)	1265	1307(67)	1253(182)
ν_2	ν sym XF_2	691 vs		678	675(220)	686(330)	808.2 vs	808.3 vs	801	802(177)	815(259)	750 br, s	757 br (3)	747	748(84)	794(119)
ν_3	δ sym F_2XO	482 m		476	486(17)	480(32)	530.4 m	529.6 s	535	549(23)	534(46)	509 ms	511 (2)	532	541(22)	509(42)
ν_4	δ sciss XF_2	332 w		330	316(0.9)	329(2.4)	377.8 w	379.5 w	372	354(3.5)	379(8.9)	378 sh	378 sh (1)	374	348(5.4)	369(6.9)
A″ ν_5	ν asym XF_2	610 s		616	583(202)	613(269)	747.0 vs	746.8 w	756	726(212)	757(277)	695 vs	696(1)	745	716(133)	776(162)
ν_6	δ asym OXF_2	351 mw		358	367(0.3)	351(5.6)	392.5 w	398.6 w	398	408(2.4)	390(9.0)	407 sh	406(2)	394	419(2.8)	382(16)

[a] Frequencies are for the solid $N(CH_3)_4^+$ salt from the present study. [b] Using empirical scaling factors of 1.0162 and 1.1650 for the stretching and deformation modes, respectively, to maximize the fit between observed and calculated frequencies. [c] Using empirical scaling factors of 1.0951 and 1.1615 for the stretching and deformation modes, respectively. [d] Using an empirical scaling factor of 0.91115 for all modes. [e] Data from refs 33–35. [f] Using empirical scaling factors of 1.0438 and 1.1840 for the stretching and deformation modes, respectively. [g] Using empirical scaling factors of 1.0996 and 1.1698 for the stretching and deformation modes, respectively. [h] Using an empirical scaling factor of 0.9006. [i] Data from ref 36. [k] Using empirical scaling factors of 0.9919 and 1.2080 for the stretching and deformation modes, respectively. [l] Using empirical scaling factors of 1.0577 and 1.2555 for the stretching and deformation modes, respectively. [m] Using an empirical scaling factor of 0.8694.

hydrolysis and HPO_2F^- becomes the sole product, as shown in eq 2

$$PF_4^- + 2H_2O \xrightarrow[20\ °C]{CH_3CN} HPO_2F^- + 3HF \qquad (2)$$

The slow hydrolysis of HPF_5^- to HPO_2F^- was verified by hydrolyzing a sample of HPF_5^- with excess water, as shown in eq 3. After 16 h at room temperature, most of the HPF_5^- had been converted to HPO_2F^-.

$$HPF_5^- + 2H_2O \xrightarrow[20\ °C]{CH_3CN} HPO_2F^- + 4HF \qquad (3)$$

Hydrolysis of $N(CH_3)_4PF_4$ in the Presence of $N(CH_3)_4F$ in CH_3CN. If the hydrolysis of PF_4^- with an equimolar amount of water is carried out in the presence of an excellent HF scavenger, such as the fluoride anion, the products are different, and POF_2^- is formed in high yield, as shown in eq 4

$$PF_4^- + H_2O + 2F^- \xrightarrow[20\ °C]{CH_3CN} POF_2^- + 2HF_2^- \qquad (4)$$

Reaction 4 is of particular interest since it provided, for the first time, a stable salt of the POF_2^- anion which previously had been observed only by either ion cyclotron resonance spectroscopy[6] or NMR spectroscopy at temperatures below -50 °C during the deprotonation of $HPOF_2$ using $[Ir(CO)H(PPh_3)_3]$.[5]

The ^{31}P NMR spectrum of a sample of $N(CH_3)_4PF_4$ at −45 °C in CH_3CN, containing a 2.6 molar excess of $N(CH_3)_4F$ and an equimolar quantity of $^{17,18}O$-enriched H_2O, is shown in Figure 4. It reveals three resonances, A, B, and C, attributable to POF_2^-,[5] PF_4^-,[4] and HPF_5^-,[10–15] respectively. The HPF_5^- was present as an impurity in the $N(CH_3)_4PF_4$ starting material and did not arise from the hydrolysis. The triplet A due to POF_2^- was significantly more intense than that in the sample of $N(CH_3)_4PF_4$ in CH_3CN alone; furthermore, the resonance exhibited a small "doublet" splitting due to the $^{16,18}O$ secondary isotopic shift, thereby providing conclusive proof that most of the POF_2^- had arisen from the hydrolysis of $N(CH_3)_4PF_4$ with the $^{17,18}O$-enriched H_2O. On warming the sample to −10 °C, the amount of POF_2^- increased further, and after warming to room temperature, complete hydrolysis of PF_4^- to POF_2^- had taken place with the $N(CH_3)_4F$ complexing the HF.

The ^{31}P NMR spectrum of the sample at 30 °C (Figure 5) shows two triplets [$^1J(^{31}P-^{19}F) = 1183$ Hz] ascribed to the two isotopomers $P^{16}OF_2^-$ and $P^{18}OF_2^-$ [$^1\Delta^{31}P(^{18,16}O) = -0.0689 \pm 0.0010$ ppm]. The observation of these two isotopomers demonstrates that the phosphorus is only bonded to one oxygen atom and identifies the POF_2^- anion. In addition, each component of the triplet is flanked by equal-intensity sextet satellites arising from coupling to ^{17}O. These satellites are highly resolved and demonstrate that there is a fortuitously small electric field gradient at the ^{17}O nucleus, and consequently the quadrupolar relaxation of the ^{17}O nucleus is very slow. Correspondingly, the ^{17}O NMR spectrum (Figure 6) displays a very sharp doublet, A, ($\Delta\nu_{1/2} = 5$ Hz) due to the $P^{17}OF_2^-$ anion. A weak resonance, B, attributable to the HPO_2F^- anion was also observed. The ^{19}F NMR spectrum at 30 °C reveals two sharp doublets arising from POF_2^- (Table 1) and HF_2^- ($\delta = -144.5$ ppm; $^1J(^{19}F-^1H) = 122$ Hz),[27] as well as some weak signals attributable to HPF_5^-.[10–15]

It should be pointed out that some of the NMR parameters of HPO_2F^- and POF_2^- exhibit a pronounced temperature and fluoride ion concentration dependence which accounts for the

(27) Christe, K. O.; Wilson, W. W. J. *Fluorine Chem.* **1990**, *46*, 339.

Table 6. Scaled LDFT Force Fields[a] for HPO_2F^- and HSO_2F

HPO_2F^-	F_{11}	F_{22}	F_{33}	F_{44}	F_{55}	F_{66}		F_{77}	F_{88}	F_{99}
A′ F_{11}	3.201						A″ F_{77}	9.405		
F_{22}	0.093	9.457					F_{88}	0.259	0.672	
F_{33}	0.086	−0.068	1.489				F_{99}	0.222	0.129	1.134
F_{44}	0.101	0.186	0.154	3.787						
F_{55}	0.124	0.071	1.387	−0.409	4.340					
F_{66}	−0.007	0.132	0.570	−0.377	2.015	2.469				

HSO_2F	F_{11}	F_{22}	F_{33}	F_{44}	F_{55}	F_{66}		F_{77}	F_{88}	F_{99}
A′ F_{11}	3.977						A″ F_{77}	11.713		
F_{22}	−0.092	11.227					F_{88}	0.259	0.738	
F_{33}	−0.029	−0.039	1.668				F_{99}	0.237	0.132	1.249
F_{44}	−0.019	−0.056	0.206	4.649						
F_{55}	−0.079	0.187	1.624	−0.370	4.909					
F_{66}	−0.031	0.156	0.667	−0.390	2.225	2.697				

[a] Stretching constants in mdyn/Å, deformation constants in mdyn Å/rad^2, and stretch-bend interaction constants in mdyn/rad. The following scaling factors were used: Stretching force constants, $(1.039)^2$; deformation constants, $(1.121)^2$; stretch-bend interaction constants, 1.039×1.121.

Table 7. Scaled[a] LDFT Force Fields for POF_2^-, SOF_2, and $ClOF_2^+$

POF_2^-	F_{11}	F_{22}	F_{33}	F_{44}		F_{55}	F_{66}
A′ F_{11}	8.338				A″ F_{55}	2.464	
F_{22}	0.344	2.886			F_{66}	0.018	1.210
F_{33}	0.118	−0.070	1.874				
F_{44}	0.024	0.045	0.478	1.631			

SOF_2	F_{11}	F_{22}	F_{33}	F_{44}		F_{55}	F_{66}
A′ F_{11}	11.120				A″ F_{55}	3.823	
F_{22}	0.203	4.293			F_{66}	0.079	1.365
F_{33}	0.156	−0.090	2.196				
F_{44}	−0.039	0.071	0.601	1.823			

$ClOF_2^+$	F_{11}	F_{22}	F_{33}	F_{44}		F_{55}	F_{66}
A′ F_{11}	10.018				A″ F_{55}	3.850	
F_{22}	−0.310	4.096			F_{66}	0.180	1.176
F_{33}	0.019	−0.045	2.212				
F_{44}	−0.121	0.138	0.563	1.717			

[a] Using the squares and the product of the scaling factors, given in Table 5, for the stretching, deformation, and stretch-bend interaction constants, respectively.

variances (see Table 1 and Figures 2 and 6) observed in some of the spectra.

Proposed Reaction Mechanism. The formation of the observed products can be rationalized by the following mechanism. (i) Pentacoordinated phosphorus compounds are thermodynamically less favorable than tetra- or hexacoordinated compounds. Consequently, they exhibit a pronounced tendency to either dismutate to tetra- and hexacoordinated compounds or add an extra molecule, such as HF or H_2O, to achieve hexacoordination. A typical example for the latter type of reaction is the addition of HF to pentacoordinated PF_4^-, counting the sterically active free valence electron pair on phosphorus in PF_4^- as a ligand, to give hexacoordinated HPF_5^-.[15,16] Similarly, it is very probable, and there is evidence for it in our ^{31}P NMR spectra (see above), that PF_4^- adds one molecule of water to form an intermediate $[HPF_4(OH)]^-$ anion which, in the absence of more information, is written here as the *cis*-isomer.

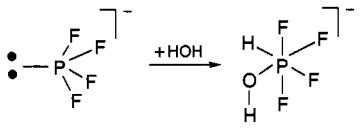

(ii) The resulting unstable $[HPF_4(OH)]^-$ anion could undergo a facile intramolecular HF elimination to give a trigonal bipyramidal $HPOF_3^-$ anion which, by analogy to the closely related POF_4^- anion,[28,29] then could undergo dismutation to a tetrahedral dioxo and an octahedral oxygen-free anion.

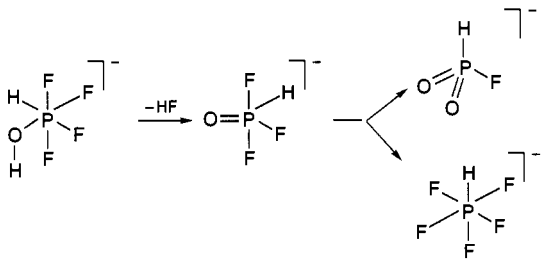

The slower hydrolysis of HPF_5^- with excess water probably involves the same mechanism with the required PF_4^- starting material being generated from HPF_5^- by HF loss. The facts that the

$$PF_4^- + HF \rightleftharpoons HPF_5^-$$

equilibrium lies far to the right and 0.5 mol of HPF_5^- is being regenerated during the hydrolysis, thus requiring many hydrolysis cycles in order to achieve a high conversion of HPF_5^- to HPO_2F^-, could explain the slowness of the HPF_5^- hydrolysis.

The exclusive formation of POF_2^- as the hydrolysis product of PF_4^- in the presence of an HF scavenger can also be explained by the same mechanism, i.e., the formation of $HPOF_3^-$ as an intermediate. However, instead of dismutating to HPO_2F^- and HPF_5^-, this anion could undergo a faster F^--promoted HF elimination to POF_2^-.

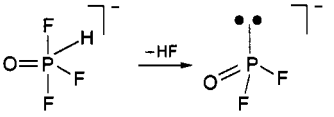

It should be emphasized that in all of the above dismutation reactions, the phosphorus central atom maintains the same formal oxidation state; i.e., in the case of PF_4^- as the starting material, all intermediates and products are phosphorus(+III) compounds and, therefore, derivatives of fluorophosphorous acids.

Methanolysis of PF_4^-. The methanolysis of PF_4^- in CH_3OH solution was also studied by NMR spectroscopy. At −40

(28) Christe, K. O.; Dixon, D. A.; Wilson, W. W.; Schrobilgen, G. J. To be published.
(29) Lustig, M.; Ruff, J. K. *Inorg. Chem.* **1967**, *6*, 2115.

Table 8. Potential Energy Distribution for HPO_2F^- and HSO_2F

	HPO_2F^-		HSO_2F	
	freq, cm^{-1}	PED, %	freq, cm^{-1}	PED, %
A′ ν_1	2352	99.8(1)	2634	99.6(1)
ν_2	1114	67.2(2) + 17.4(3) + 10.8(6) + 4.5(4)	1220	65.4(2) + 16.7(3) + 11.6(6) + 5.8(4)
ν_3	1006	81.1(3) + 18.6(5)	1095	80.4(3) + 19.3(5)
ν_4	728	90.4(4) + 5.0(5) + 4.0(6) + 0.4(2)	803	89.1(4) + 6.7(5) + 3.0(6) + 1.0(2)
ν_5	550	49.2(5) + 40.9(6) + 8.4(3) + 1.1(4)	603	46.6(5) + 40.5(6) + 10.6(3) + 1.8(4)
ν_6	425	76.8(6) + 16.3(3) + 5.2(5) + 1.7(4)	466	78.3(6) + 14.7(3) + 5.5(5) + 1.5(4)
A″ ν_7	1342	69.3(7) + 20.0(8) + 10.7(9)	1485	69.2(7) + 19.8(8) + 11.0(9)
ν_8	1023	99.8(8)	1121	99.9(8)
ν_9	384	93.2(9) + 6.8(8)	417	94.0(9) + 6.0(8)

Table 9. Potential Energy Distributions for POF_2^-, SOF_2, and $ClOF_2^+$

	POF_2^-		SOF_2		$ClOF_2^+$	
	freq, cm^{-1}	PED, %	freq, cm^{-1}	PED, %	freq, cm^{-1}	PED, %
A′ ν_1	1158	89.8(1) + 7.9(3) + 1.3(2) + 1(4)	1333	88.5(1) + 7.3(3) + 2.6(2) + 1.6(4)	1265	86.2(1) + 6.0(3) + 5.4(2) + 2.4(4)
ν_2	678	73.7(2) + 13.5(4) + 12.7(3)	801	76.0(2) + 12.7(4) + 11.2(3)	747	80.7(2) + 9.8(4) + 8.4(3) + 1.1(1)
ν_3	476	84.1(3) + 9.7(2) + 5.9(4)	535	86.8(3) + 7.4(4) + 5.7(2)	532	91.8(3) + 5.2(4) + 2.8(2)
ν_4	330	78.6(4) + 20.9(3) + 0.5(2)	372	78.7(4) + 21.0(3) + 0.2(2)	374	83.7(4) + 16.1(3)
A″ ν_5	616	84.5(5) + 15.5(6)	756	84.8(5) + 15.2(6)	745	86.7(5) + 13.3(6)
ν_6	358	97.7(6) + 2.3(5)	398	99.0(6) + 1.0(5)	394	99.8(6)

°C, the main reaction product was $PF_2(OCH_3)$[26,30,31] [^{31}P: triplet [$^1J(^{31}P-^{19}F)$ = 1286 Hz] of quartets [$^3J(^{31}P-^1H)$ = 8.2 Hz] at δ = 113.2], while after a brief warming to room temperature, $PF(OCH_3)_2$[30] [^{31}P: doublet [$^1J(^{31}P-^{19}F)$ = 1202 Hz] of septets [$^3J(^{31}P-^1H)$ = 10 Hz] at δ = 132.9] became also a major product.

$$PF_4^- + CH_3OH \xrightarrow[-40\ °C]{CH_3OH} PF_2(OCH_3) + HF_2^- \quad (5)$$

$$PF_2(OCH_3) + CH_3OH \xrightarrow[20\ °C]{CH_3OH} PF(OCH_3)_2 + HF \quad (6)$$

In addition to these two phosphorous acid methyl esters, a small amount of a phosphorus(+V) byproduct was observed which is attributed to $OPF(OCH_3)_2$ [^{31}P: doublet [$^1J(^{31}P-^{19}F)$ = 712 Hz] of septets [$^3J(^{31}P-^1H)$ = 12 Hz] at δ = 13.6], which could arise from methanolysis of PF_3O.

Ab Initio Calculations and Vibrational Spectra. Since the HPO_2F^- and POF_2^- anions had previously been only partially characterized, it was of interest to analyze their vibrational spectra (Figures 7 and 8 and Tables 4 and 5) and force fields with the help of *ab initio* calculations (Tables 2–10). For comparison, the geometries and vibrational spectra of the isoelectronic sulfur compounds, HSO_2F and SOF_2, were also calculated. Since the known SOF_2 molecule has been well-characterized,[32–34] its experimental data can be used to test the quality of our calculations which were done at the local density functional (LDFT), nonlocal density functional (NLDFT/TZVP), and Hartree–Fock (HF/DZP$^+$) levels of theory. As can be seen from Table 3, the HF/DZP$^+$ calculation predicts best the experimental geometry of SOF_2,[32] and the resulting bond lengths are slightly shorter than the experimentally observed ones. As expected, the density functional theory calculations can predict well the bond angles, but the resulting bond lengths are about 0.05 Å longer than the experimentally observed ones. Another test for the quality of our calculations is a comparison of the calculated and observed vibrational frequencies. As can be seen from Tables 4 and 5, the LDFT frequencies, after appropriate scaling to compensate for the overestimation of the bond lengths, yield the best prediction of the experimentally observed values and establish their assignments. The calculated force fields and potential energy distributions are given in Tables 6–9. The valence force constants are summarized in Table 10 and show that within the XOF_2 series, SOF_2 exhibits the strongest bonds and that the bonds in HXO_2F are stronger than those in the corresponding XOF_2 species which is in line with the calculated bond lengths.

Table 10. Valence Force Constants (mdyn/Å) of POF_2^-, SOF_2, $ClOF_2^+$, HPO_2F^-, and HSO_2F

	POF_2^-	SOF_2	$ClOF_2^+$	HPO_2F^-	HSO_2F
f_{XO}	8.34	11.12	10.02	9.43	11.47
f_{XF}	2.68	4.06	3.97	3.79	4.65
f_{XH}				3.20	3.98

The successful synthesis of a stable POF_2^- salt is in accord with the well-known stabilities of the isoelectronic species SOF_2, PF_3, SO_2F^-, and SF_3^+, all of which possess 26 valence electrons and a previous value of 56 ± 4 kcal/mol for the F^- affinity of POF, determined by ion cyclotron resonance spectroscopy.[6] The relative F^- affinities of the various phosphorus species involved in the present study (7a) were obtained by subtracting the

$$A + F^- \rightarrow AF^- \quad (7a)$$

$$COF_3^- \xrightarrow{42.6\ kcal/mol} COF_2 + F^- \quad (7b)$$

$$A + COF_3^- \xrightarrow{\Delta H} AF^- + COF_2 \quad (7c)$$

experimentally known[6] value of 42.6 kcal/mol for (7b) from the reaction enthalpies, ΔH, of (7c) which were calculated from the total energies of their components using the DZP$^+$ basis set. The results are summarized in Table 11 and agree well with the available experimental data.[6]. Table 11 shows that all these molecules possess sufficiently high F^- affinities for the formation of stable salts and that FPO and HPO_2 are stronger

(30) Cameron, J. H.; McLennan, A. J.; Rycroft, D. S.; Winfield, J. M. *J. Fluorine Chem.* **1981**, *19*, 135 and references cited therein. Reddy, G. A.; Schmutzler, R. *Z. Naturforsch.* **1970**, *25b*, 1199.
(31) Kwiatkowski, J. S.; Leszczynski, J. *J. Mol Struct.* **1992**, *258*, 287 and references cited therein.
(32) Lucas, N. J. D.; Smith, J. G. *J. Mol. Spectrosc.* **1972**, *43*, 327.
(33) Boyd, R. J.; Szabo, J. P. *Can. J. Chem.* **1982**, *60*, 730.
(34) (a) Shimanouchi, T. *J. Phys. Chem. Ref. Data* **1977**, *6*, 993. (b) Pace, E. L.; Samuelson, H. V. *J. Chem. Phys.* **1966**, *44*, 3682.
(35) O'Hara, T. J.; Noftle, R. E. *J. Fluorine Chem.* **1982**, *20*, 149.
(36) Christe, K. O.; Curtis, E. C.; Schack, C. J. *Inorg. Chem.* **1972**, *11*, 2212.

Table 11. Calculated and Experimental F^- Affinities of Various Phosphorus Fluorides and HF

	F affinity (kcal/mol)	
molecule	calcd	exp[a]
PF_3	41.0	40
HF	41.1	39
POF_3	52.3	48
FPO	59.0	56
HPF_4	73.5	
HPO_2	79.9	
PF_5	87.3	85

[a] Data from ref 6.

Lewis acid than either PF_3, HF, POF_3, or SO_2 (F^- affinity of SO_2 = 44 kcal/mol).[6]

The reaction enthalpies of the hydrolysis reactions of HPF_5^- and of PF_4^- with either equimolar amounts or excess of H_2O were also estimated from the heats of formation of the gaseous species calculated with the DZP+ basis set. As can be seen from the Born Haber cycle (8), the calculated values for the two paths are practically identical, thus demonstrating the

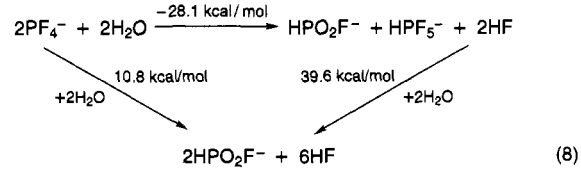

(8)

consistency of these calculations. The endothermicity of the hydrolysis of HPF_5^- is also in accord with the experimentally observed slowness of this reaction.

Acknowledgment. We thank the U. S. Air Force Phillips Laboratory (K.O.C., G.J.S.), the U.S. Army Research Office (K.O.C.), and the Natural Sciences and Engineering Research Council of Canada (G.J.S.) for financial support.